

Deep Learning in Medical Image Analysis: Techniques for Classification and Segmentation

Tutorial of EE4211

Department of Electrical Engineering
City University of Hong Kong
06/11/2020

➤ WCE Image Classification

- Densely Connected Convolutional Networks (CVPR 2017)
- Triple ANet: Adaptive abnormal-aware attention network for WCE image classification (MICCAI 2019)

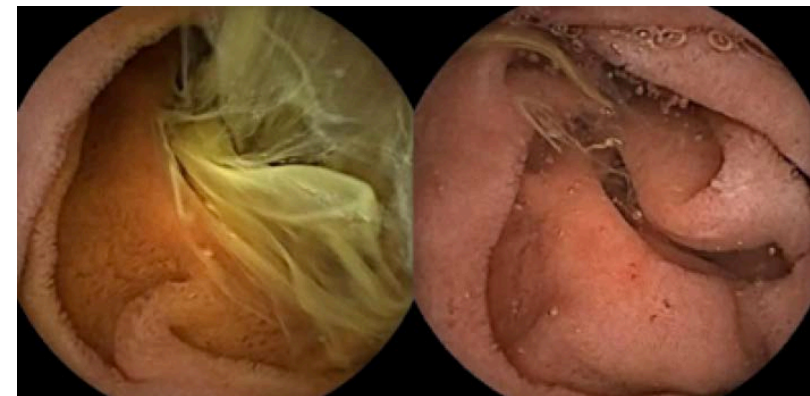
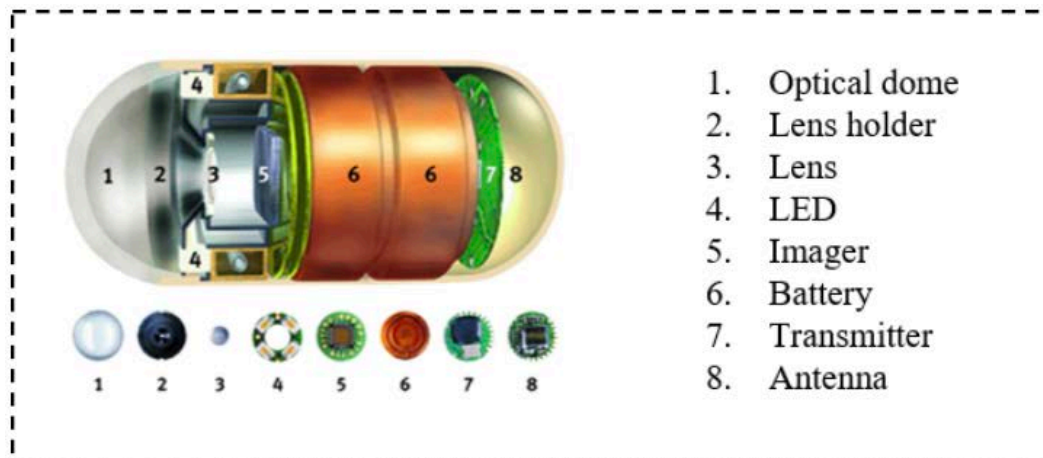
➤ COVID-19 CT Image Segmentation

- U-Net: Convolutional Networks for Biomedical Image Segmentation (MICCAI 2015)
- Inf-Net: Automatic COVID-19 Lung Infection Segmentation From CT Images (IEEE TMI 2020)

➤ WCE Image Classification

- Densely Connected Convolutional Networks (CVPR 2017)
- Triple ANet: Adaptive abnormal-aware attention network for WCE image classification (MICCAI 2019)

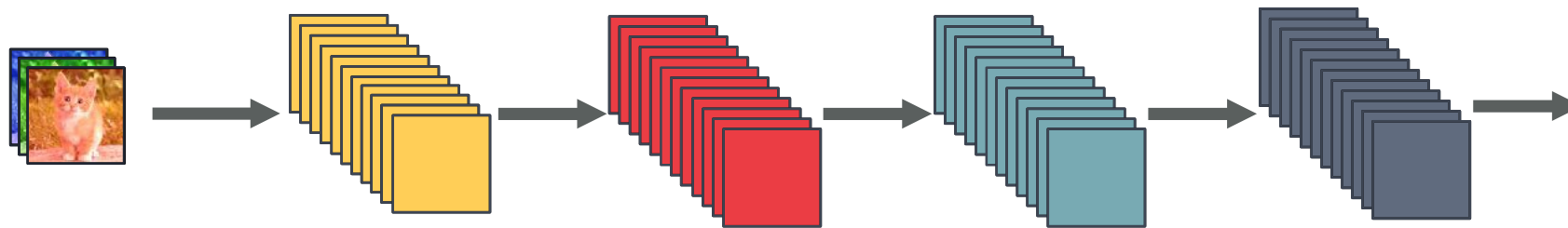
– WCE denotes “Wireless Capsule Endoscopy”



CONVOLUTIONAL NETWORKS

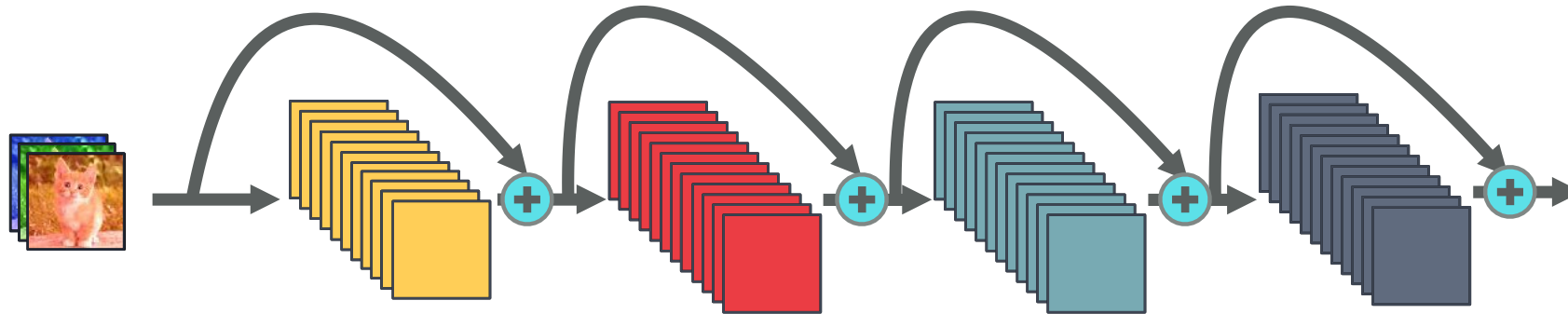


Standard Connectivity



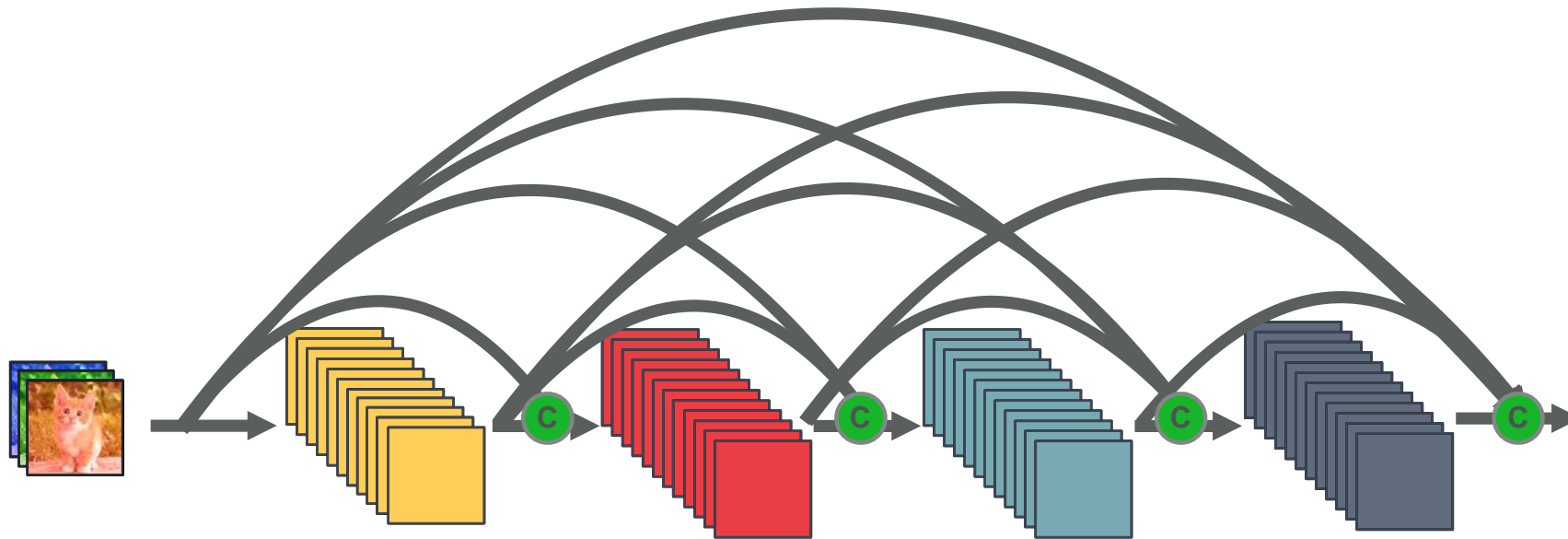
ResNet Connectivity

Identity mappings promote gradient propagation.



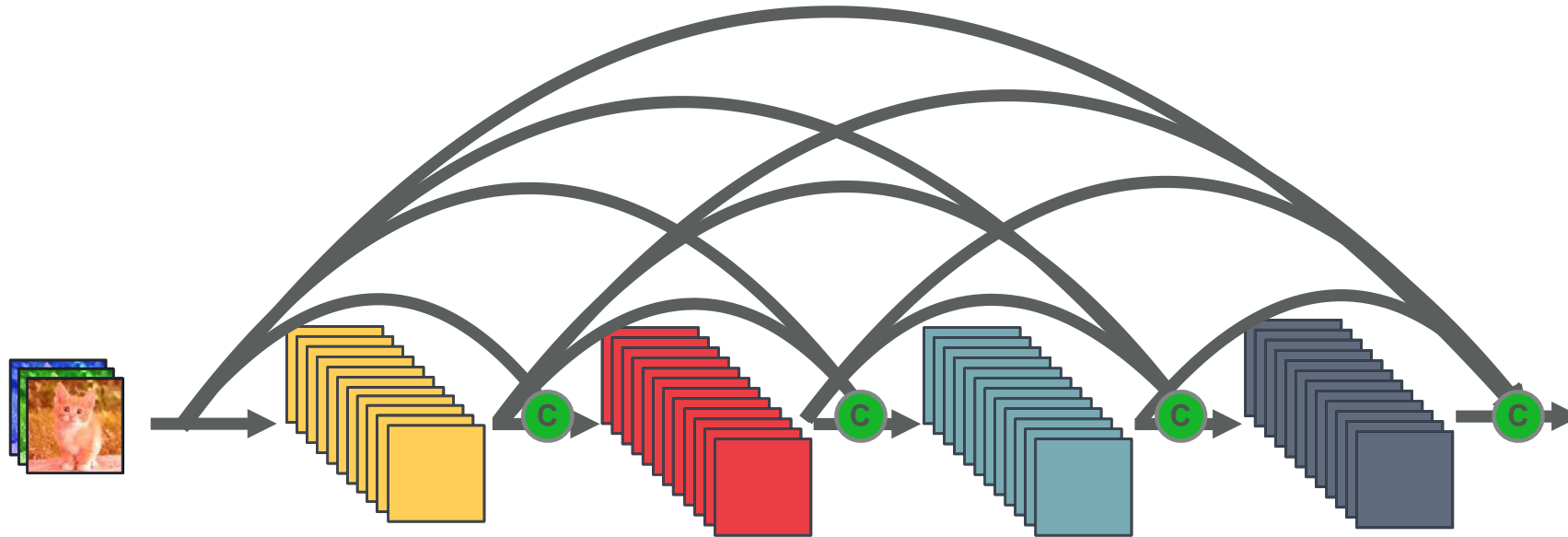
 : Element-wise
addition

Dense Connectivity



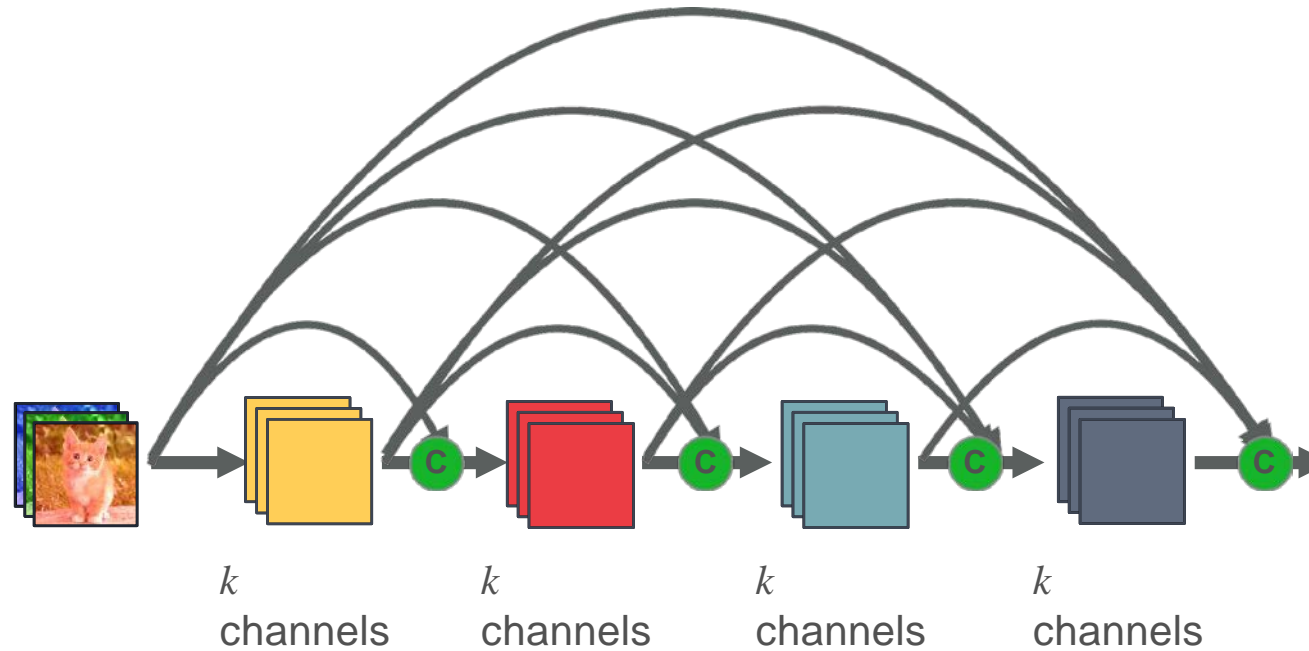
 : Channel-wise
concatenation

Dense and Slim



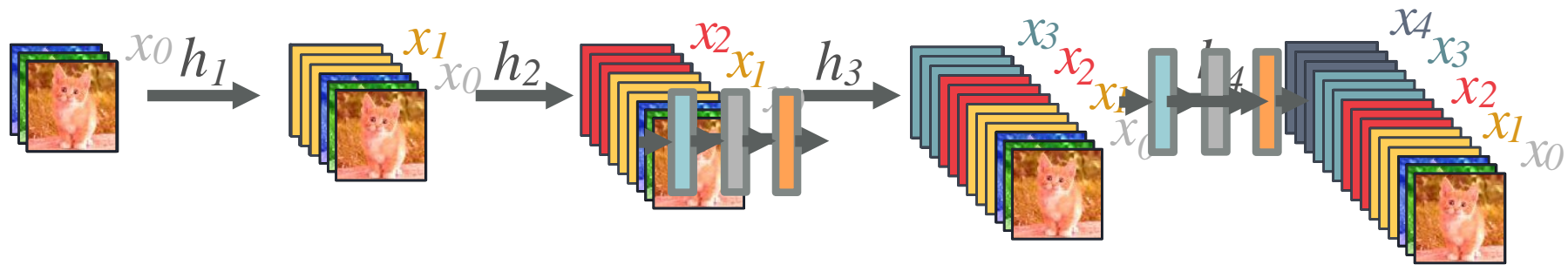
 : Channel-wise
concatenation

Dense and Slim

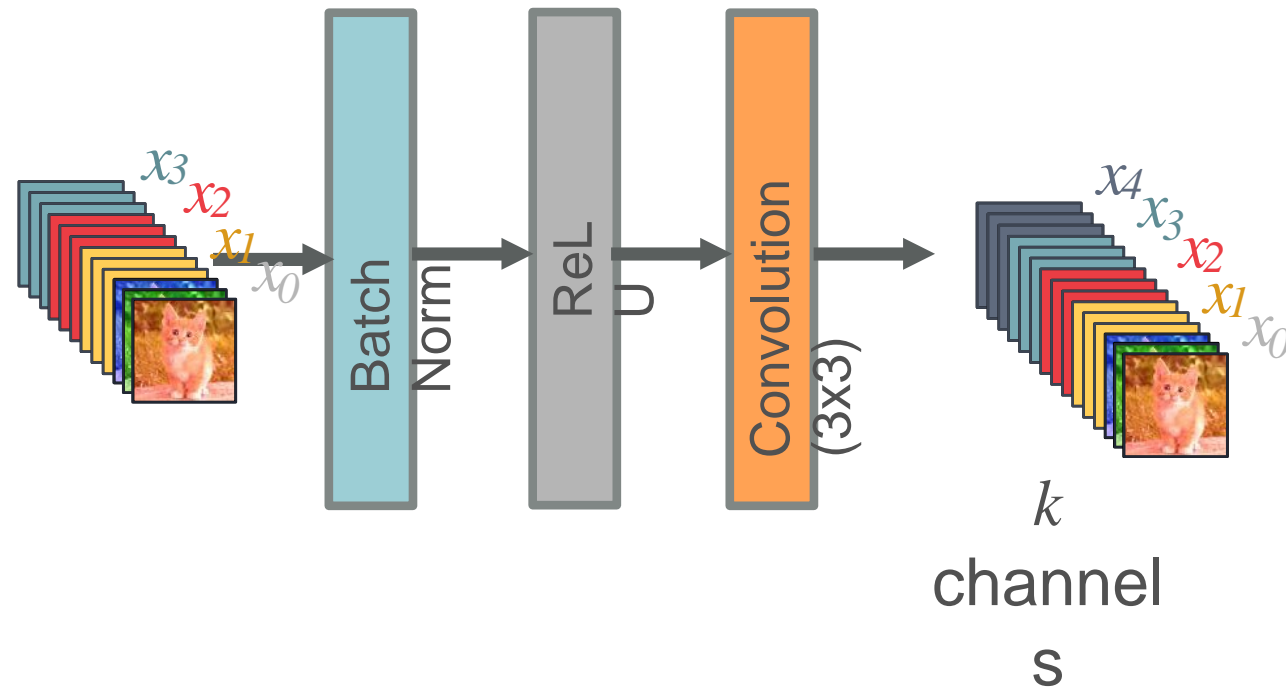


k : Growth
Rate

Forward Propagation of Dense Block



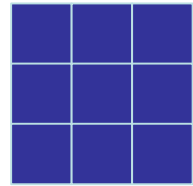
Composite Layer in DenseNet



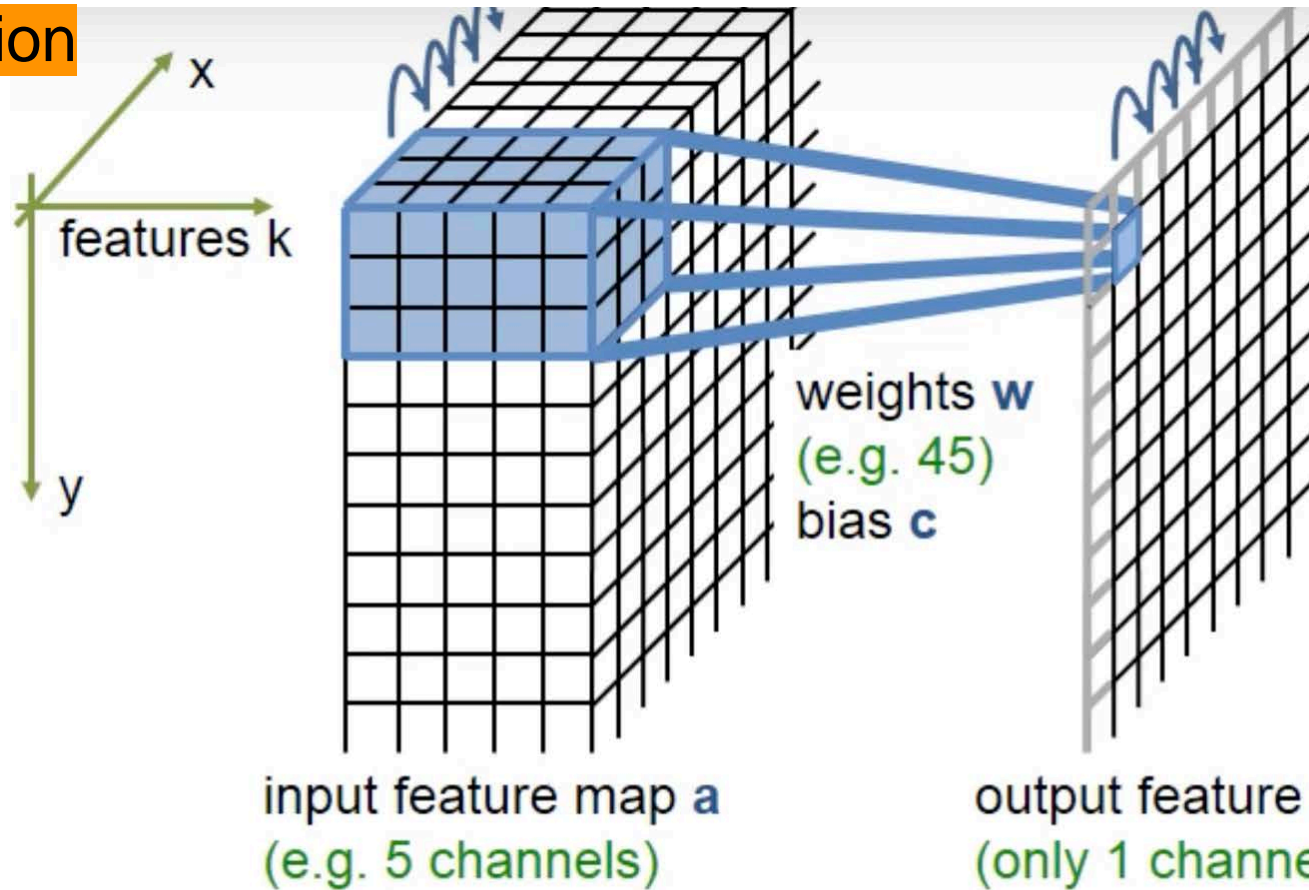
$$x_5 = h_5([x_0, \dots, x_4])$$

WCE Image Classification

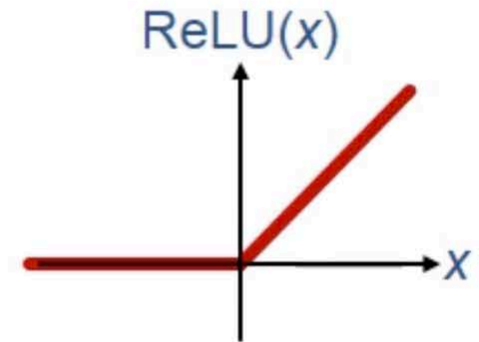
Convolution



3x3 kernel

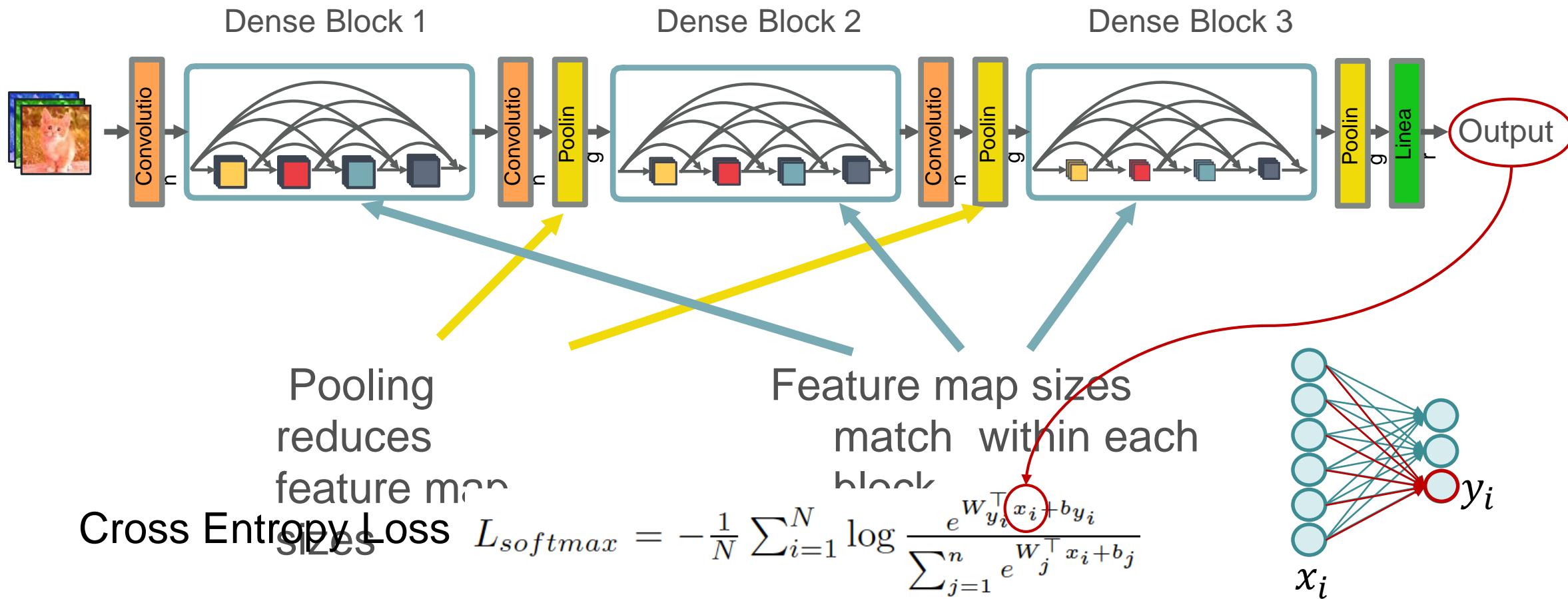


- Only valid part of convolution is used.
- For 3x3 convolutions a 1-pixel border is lost



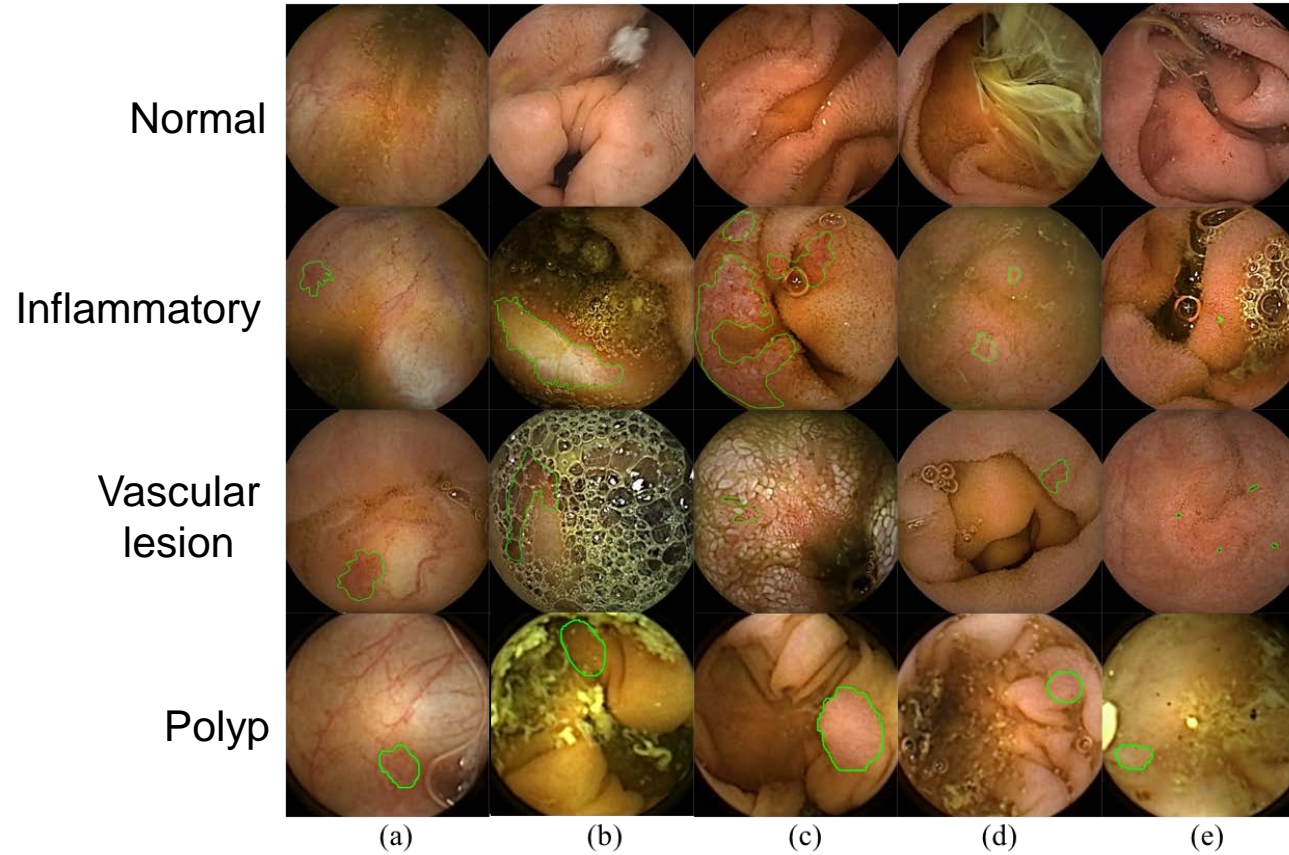
$$b_{x,y,l} = \text{ReLU} \left(\sum_{\substack{i \in \{-1,0,1\} \\ j \in \{-1,0,1\} \\ k \in \{1,\dots,K\}}} w_{i,j,k,l} \cdot a_{x+i,y+j,k} + c_l \right)$$

DenseNet



WCE Image Classification

Main Difficulties

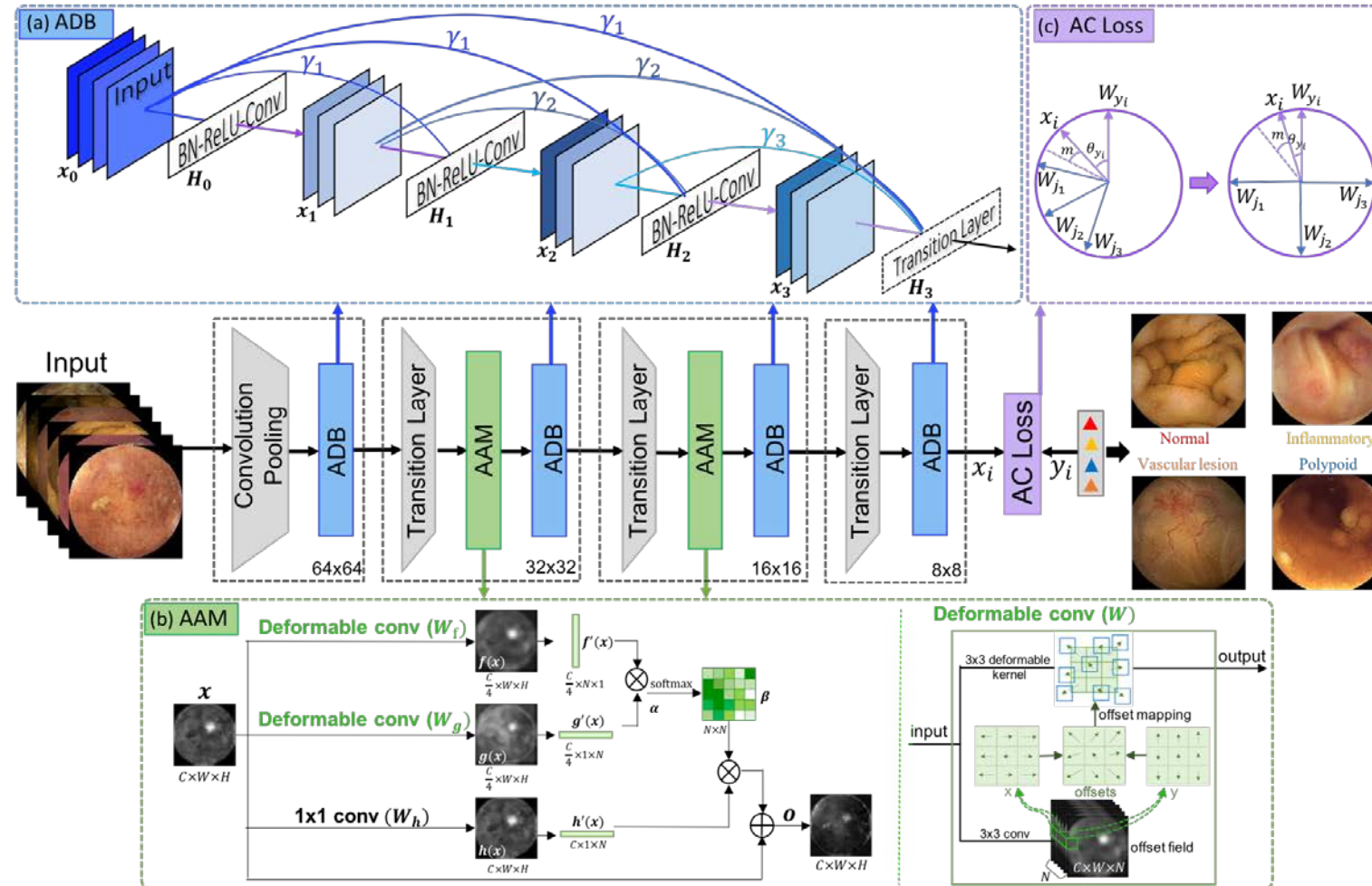


Diverse characteristics

- 1, huge intra-class variances
- 2, high degree of inter-class visual similarities

WCE Image Classification

Framework



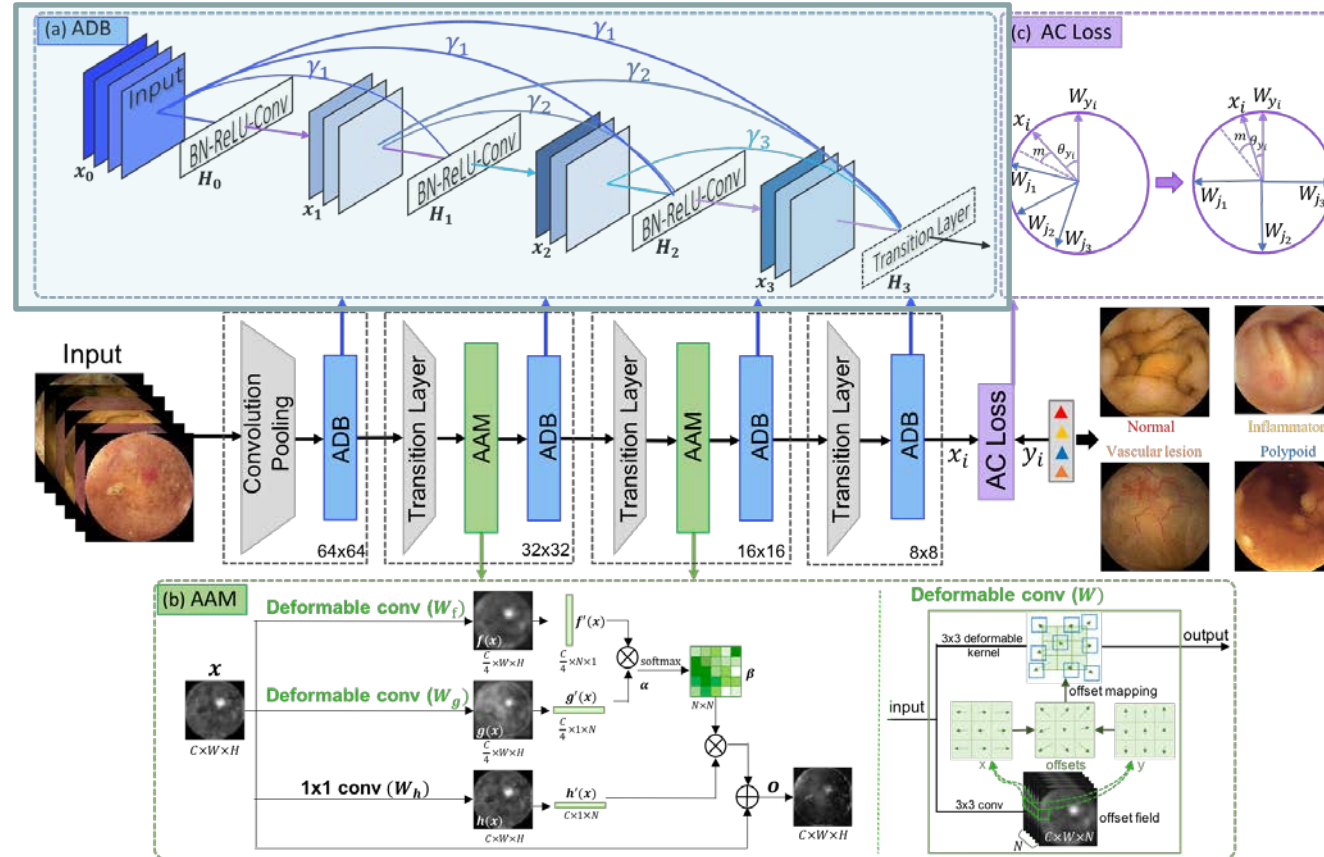
- **ADB:**
Adaptive Dense Block

- **AAM:**
Abnormal-aware Attention Module

- **AC Loss:**
Angular Contrastive Loss

WCE Image Classification

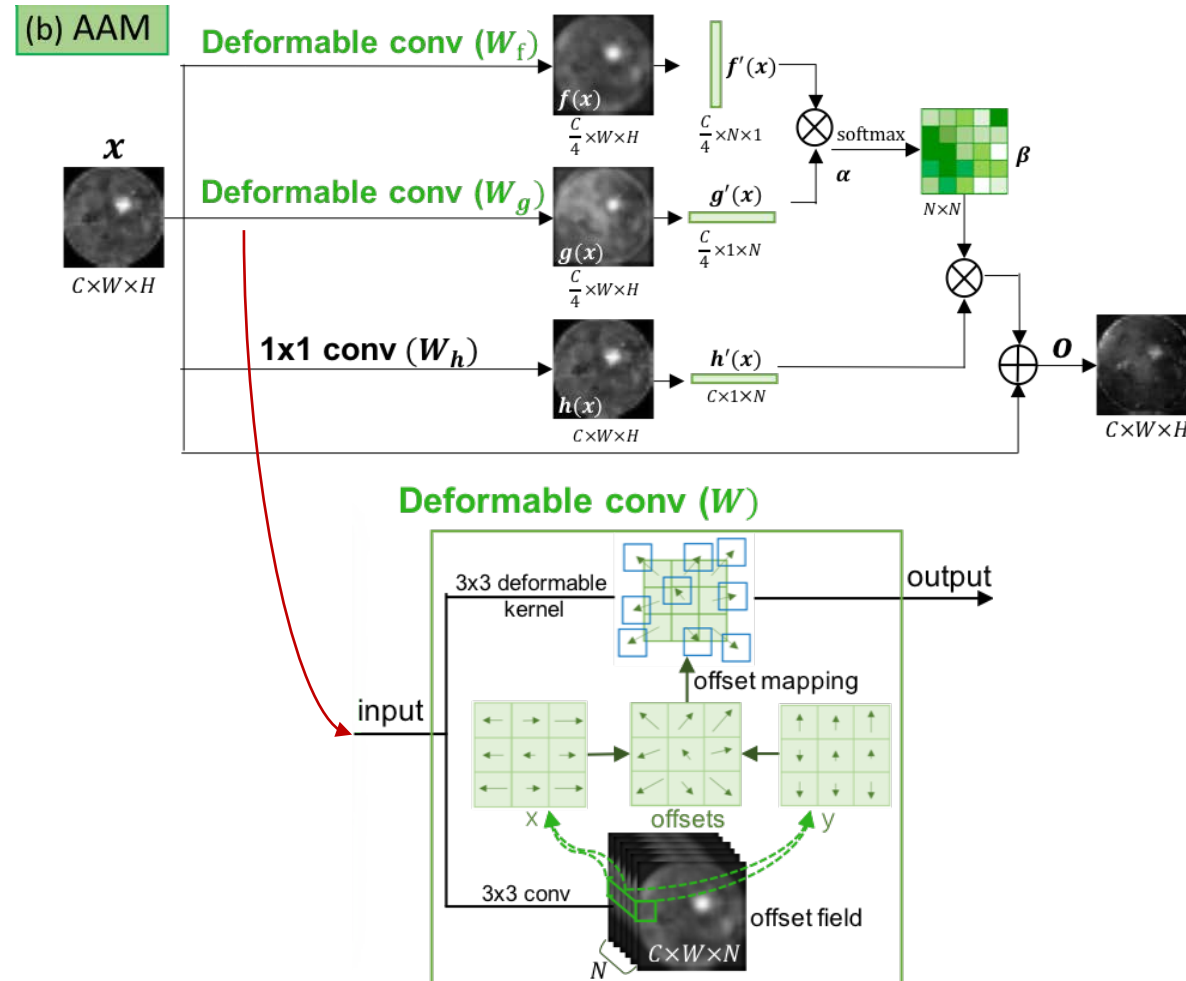
ADB: Adaptive Dense Block



Let x_l denote output of l^{th} layer and γ_l is its corresponding weight scalar, adaptive dense connectivity is formulated as $x_l = H_l([\gamma_0 x_0, \gamma_1 x_1, \dots, \gamma_{l-1} x_{l-1}])$. $H_l(\cdot)$ is a composite function with BN, ReLU and Conv, and each $H_l(\cdot)$ produces $k = 12$ feature maps.

WCE Image Classification

AAM: Abnormal-aware Attention Module



WCE Image Classification

AC Loss: Angular Contrastive Loss

$$L_{softmax} = -\frac{1}{N} \sum_{i=1}^N \log \frac{e^{W_{y_i}^\top x_i + b_{y_i}}}{\sum_{j=1}^n e^{W_j^\top x_i + b_j}}$$

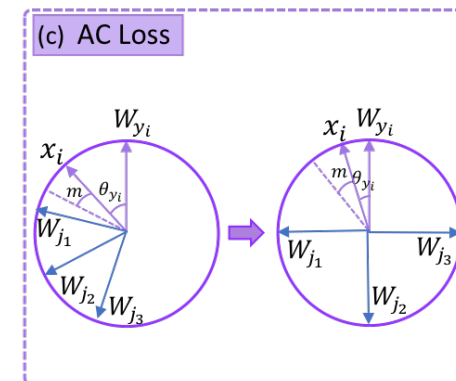
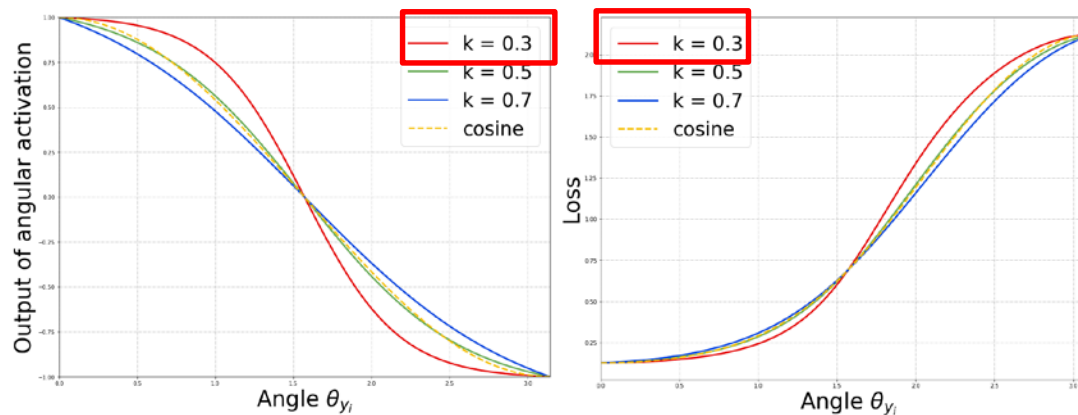
$$F(W_j, x_i) = \|W_j\| \cdot \|x_i\| \cos \theta_j \quad \Downarrow \quad \|x_i\| = 1 \quad \|W_j\| = 1$$

$$L_{cosine} = -\frac{1}{N} \sum_{i=1}^N \log \frac{e^{s \cos \theta_{y_i}}}{\sum_{j=1}^n e^{s \cos \theta_j}}$$

$$F(W_j, x_i) = s \|W_j\| \cdot \|x_i\| \cdot A(\theta_j) \quad \Downarrow$$

$$L_{AC} = -\frac{1}{N} \sum_{i=1}^N \log \frac{e^{s A(\theta_{y_i} + m)}}{e^{s A(\theta_{y_i} + m)} + \sum_{j \neq y_i}^n e^{s A(\theta_j)}} + \frac{1}{n} \cdot \frac{1}{n-1} \sum_{y_i=1}^n \sum_{j \neq y_i}^n W_{y_i}^\top W_j$$

$$A(\theta_j) = \frac{1 + e^{(-\frac{\pi}{2k})}}{1 - e^{(-\frac{\pi}{2k})}} \cdot \frac{1 - e^{(\frac{\theta_j}{k} - \frac{\pi}{2k})}}{1 + e^{(\frac{\theta_j}{k} - \frac{\pi}{2k})}}$$



WCE Image Classification

Results

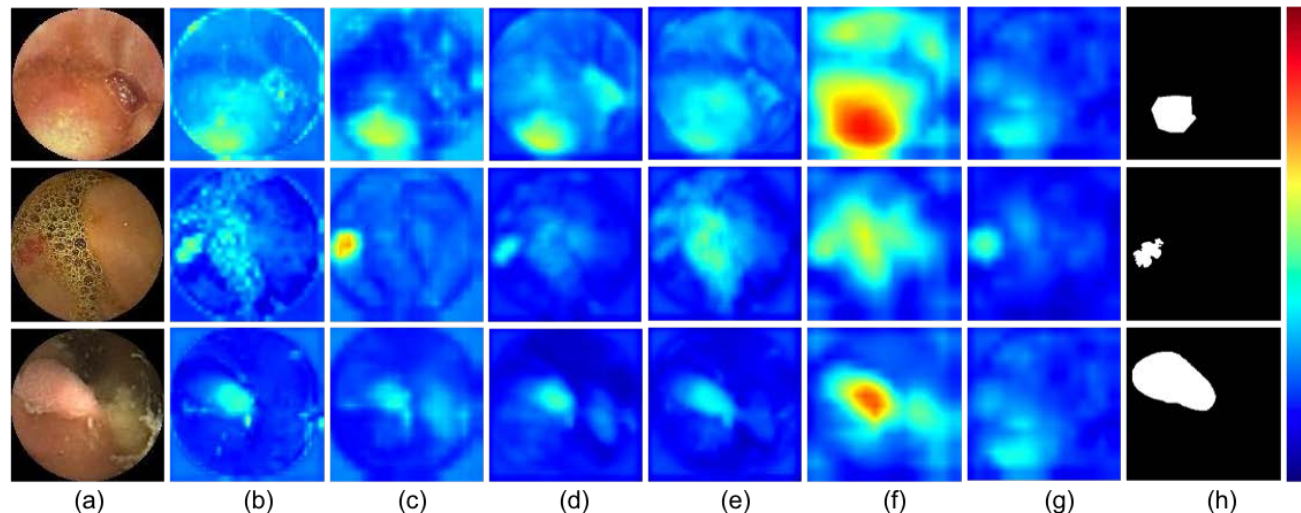
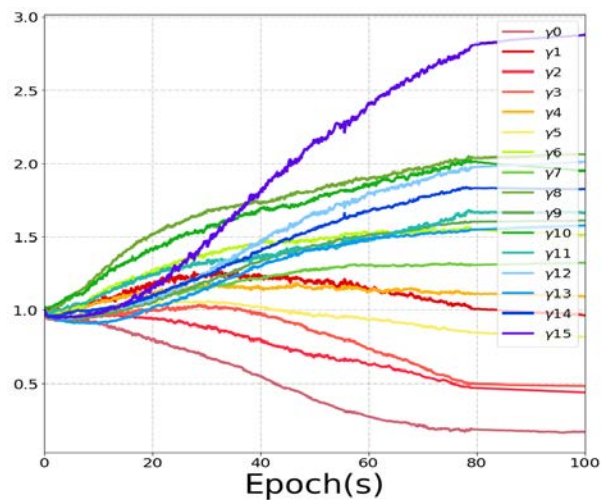
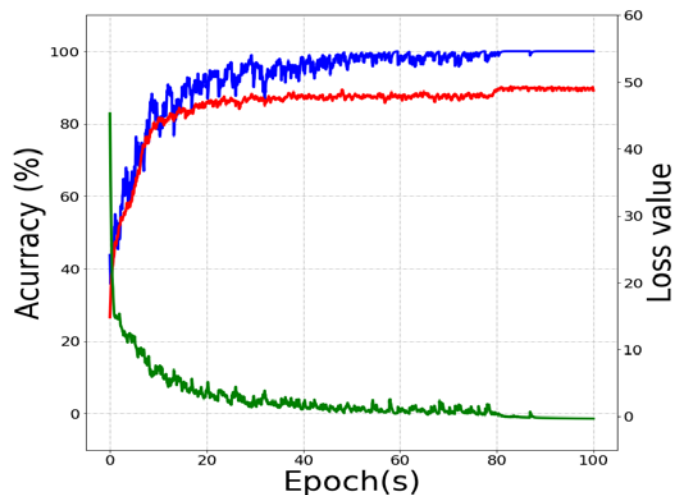
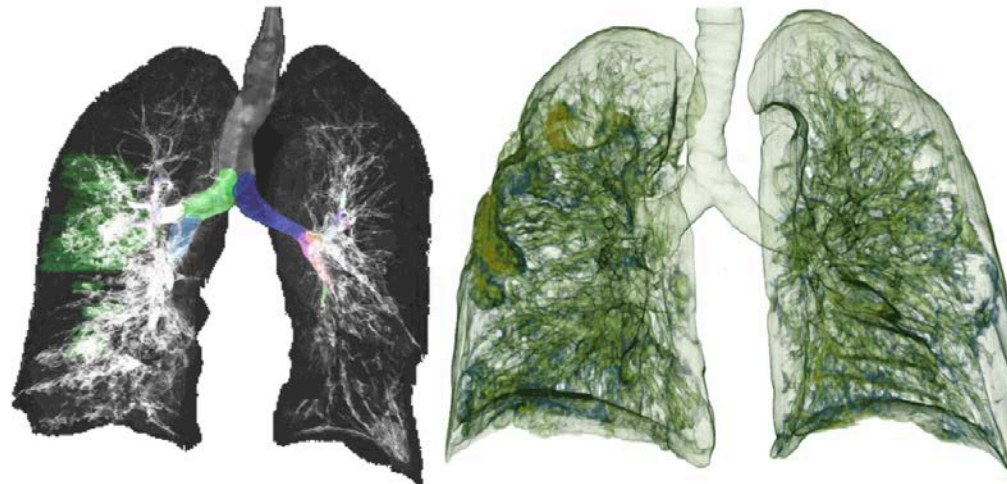


Table 1: Comparison results for WCE image classification. w/ ADB, w/ AAM and w/ AC Loss denote DenseNet with ADB (instead of original dense block), DenseNet with AAM and DenseNet minimized by AC Loss (instead of original softmax cross entropy loss), respectively.

Methods	Normal ACC(%)	Inflammatory ACC(%)	Vascular lesion ACC(%)	Polyp ACC(%)	OA	Cohen's Kappa
DenseNet [4]	92.69±0.49	90.12±0.54	93.71±0.52	97.59±0.39	87.05±0.45	82.66±0.60
w/ ADB	93.03±0.40	89.94±0.18	93.61±0.15	97.71±0.27	87.14±0.21	82.78±0.28
w/ AAM	94.06±0.17	91.49±0.81	94.47±0.77	97.78±0.42	88.89±0.52	85.13±0.69
w/ AC Loss	93.59±0.30	91.20±0.33	94.94±0.34	97.69±0.46	88.70±0.20	84.87±0.27
Triple ANet	94.03±0.09	91.73±0.29	95.26±0.33	97.81±0.20	89.41±0.23	85.82±0.31
Fan et al. [3]	85.44±1.43	83.09±0.79	90.19±0.96	95.47±0.89	77.10±1.14	69.30±1.58
Jia et al. [5]	86.16±1.07	83.37±0.71	90.32±0.88	95.81±0.59	77.83±1.28	70.31±1.74
Seguí et al. [7]	92.11±0.60	89.71±0.48	94.21±0.57	97.31±0.12	86.67±0.84	82.15±1.12
Yuan et al. [9]	93.44±0.30	90.79±0.26	93.91±0.17	97.73±0.35	87.93±0.07	83.84±0.08

➤ COVID-19 CT Image Segmentation

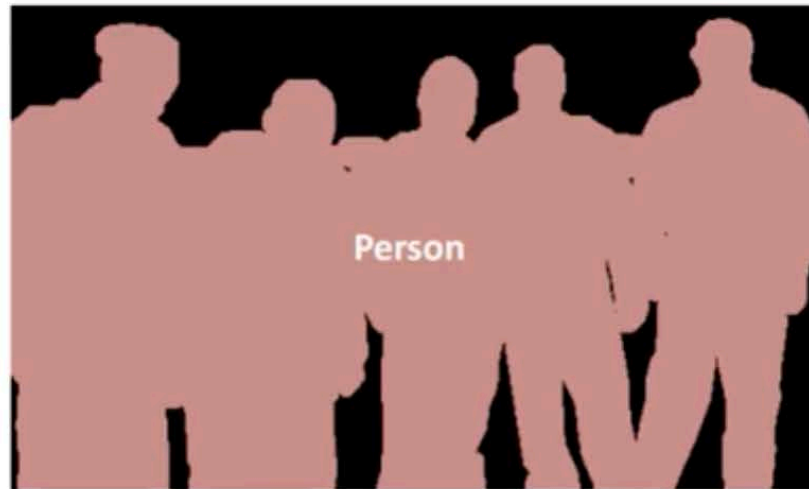
- U-Net: Convolutional Networks for Biomedical Image Segmentation (MICCAI 2015)
- Inf-Net: Automatic COVID-19 Lung Infection Segmentation From CT Images (IEEE TMI 2020)
 - Automated detection of lung infections from computed tomography (CT) images offers a great potential for the diagnosis of COVID-19



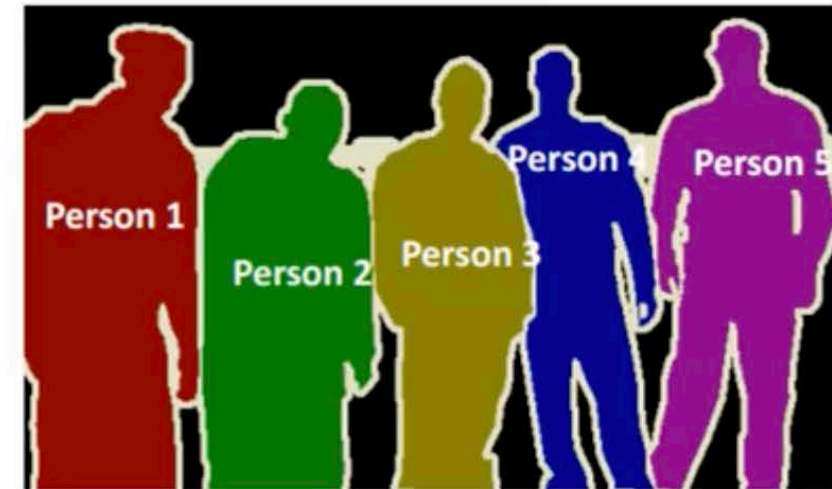
COVID-19 CT Image Segmentation



Object Detection

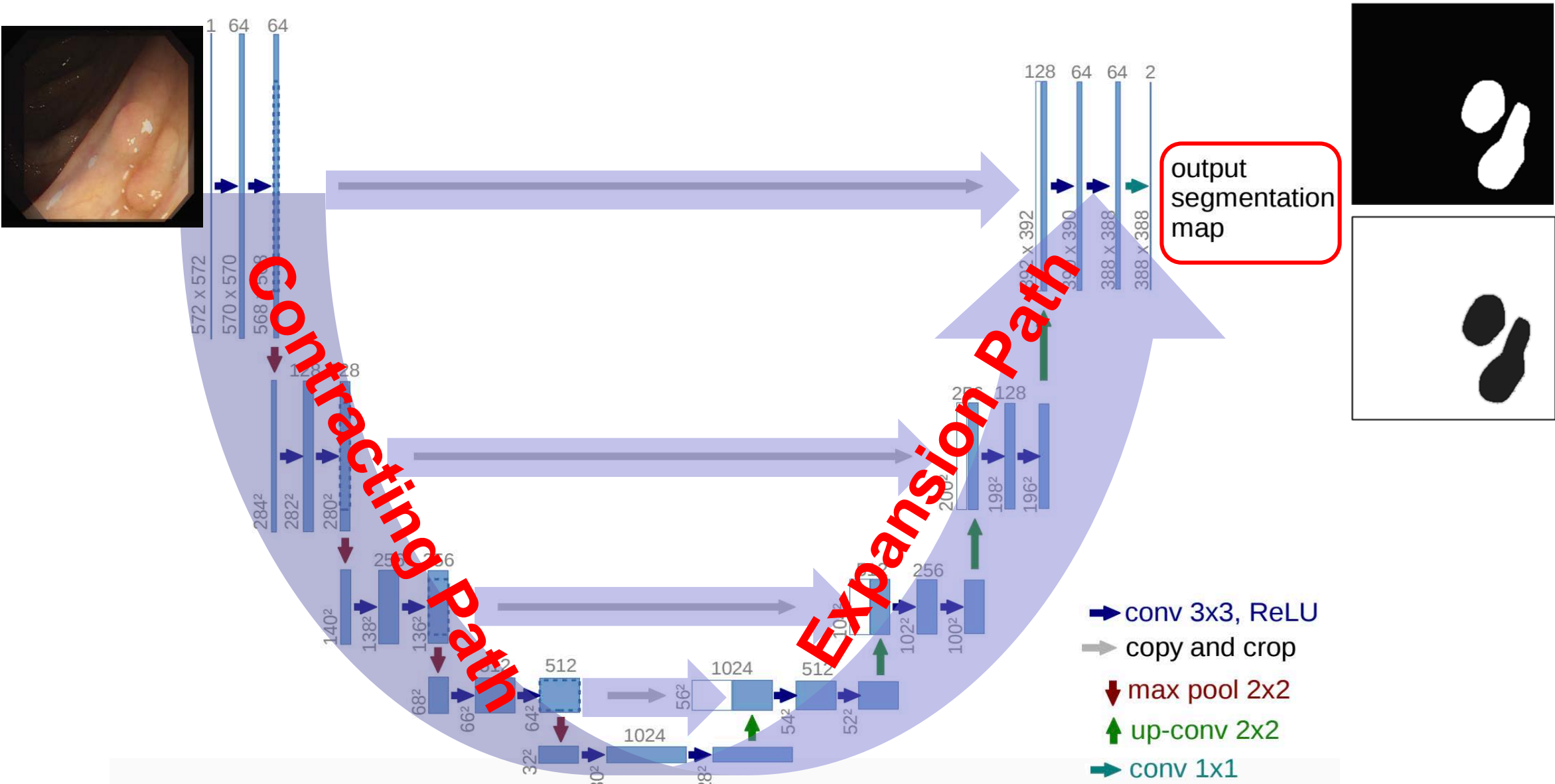


Semantic Segmentation



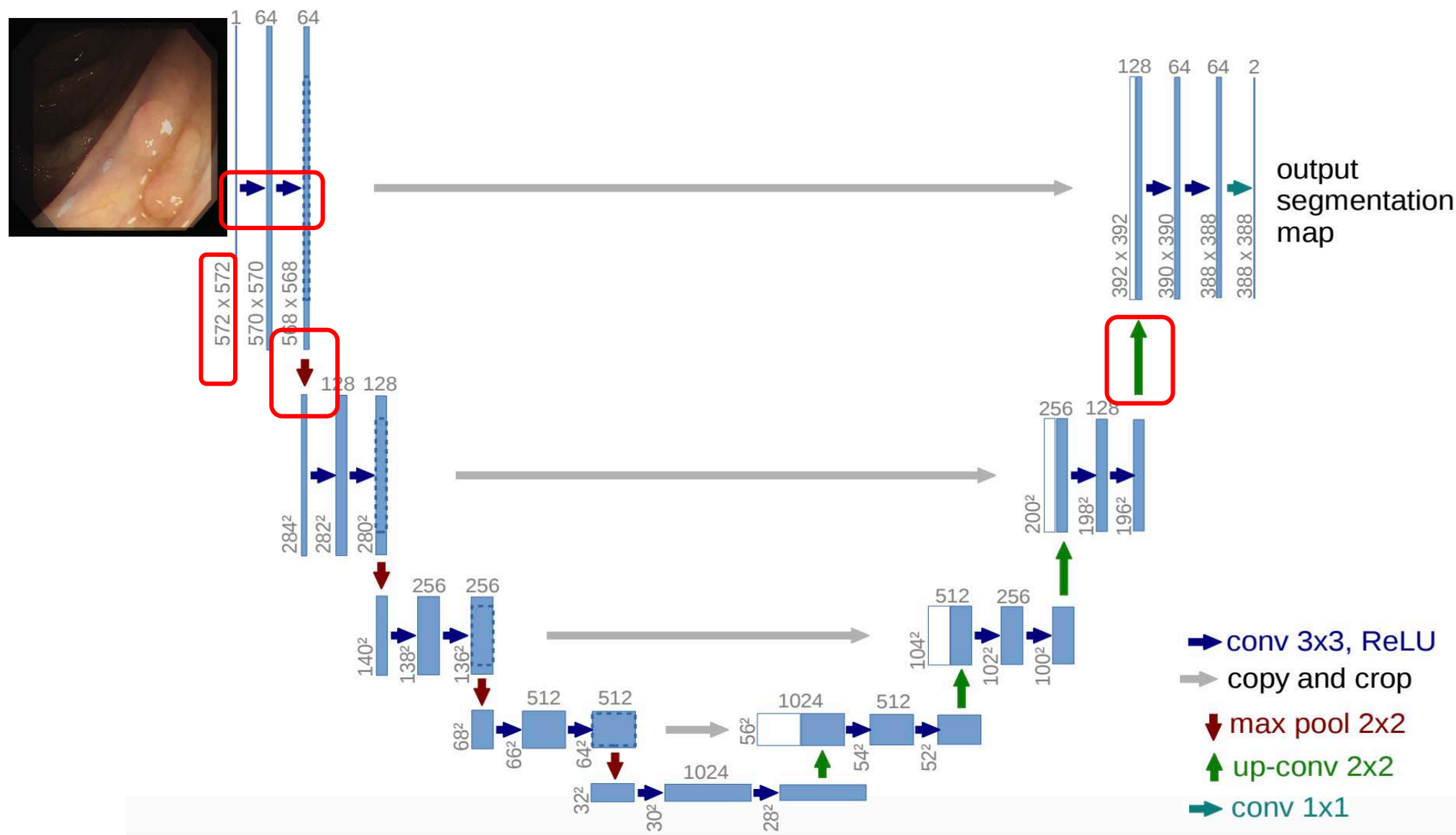
Instance Segmentation

COVID-19 CT Image Segmentation



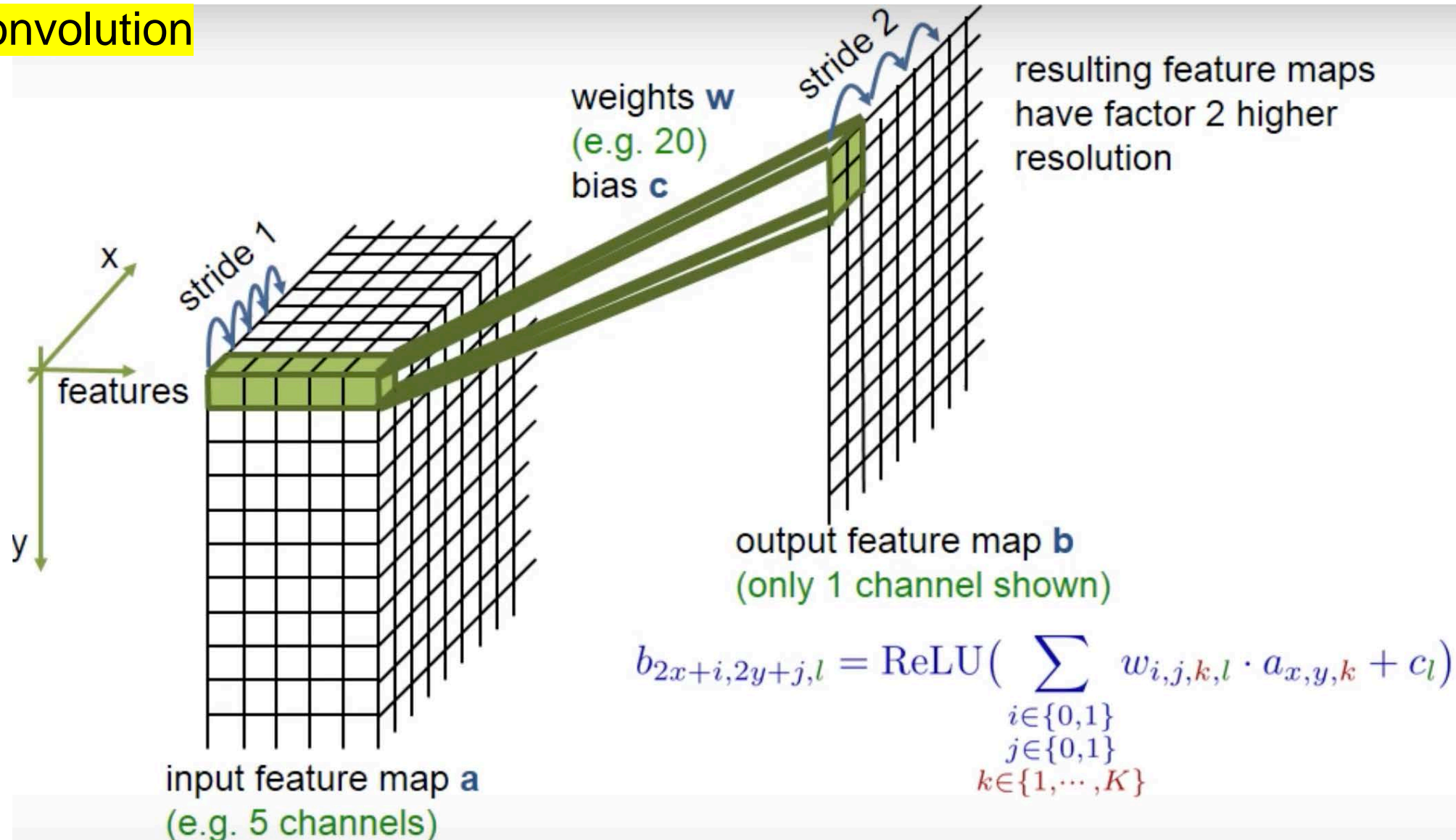
Ronneberger, Olaf, Philipp Fischer, and Thomas Brox. "U-net: Convolutional networks for biomedical image segmentation." MICCAI, 2015.

COVID-19 CT Image Segmentation

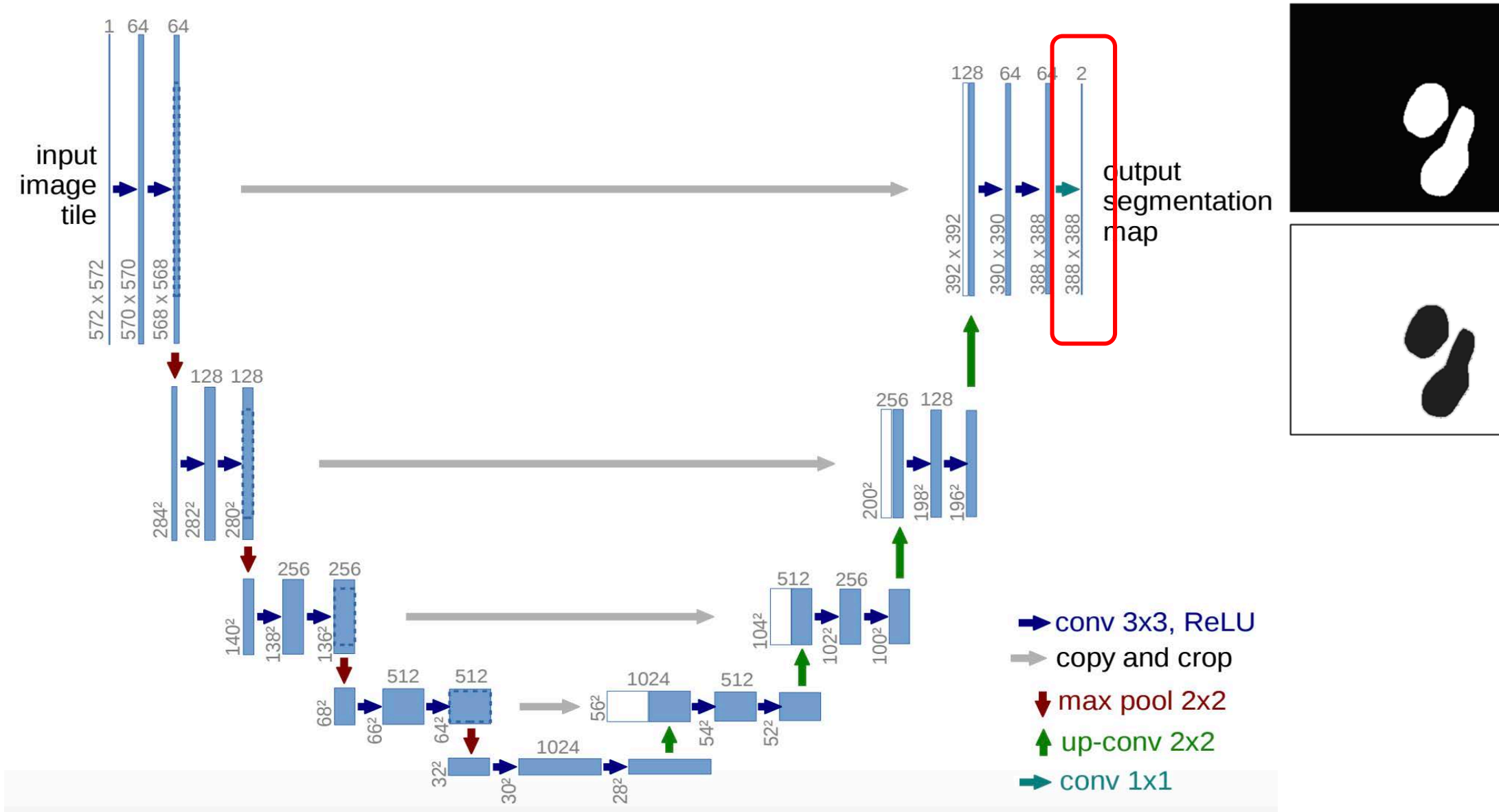


Ronneberger, Olaf, Philipp Fischer, and Thomas Brox. "U-net: Convolutional networks for biomedical image segmentation." MICCAI, 2015.

Up Convolution



COVID-19 CT Image Segmentation



Ronneberger, Olaf, Philipp Fischer, and Thomas Brox. "U-net: Convolutional networks for biomedical image segmentation." MICCAI, 2015.

COVID-19 CT Image Segmentation

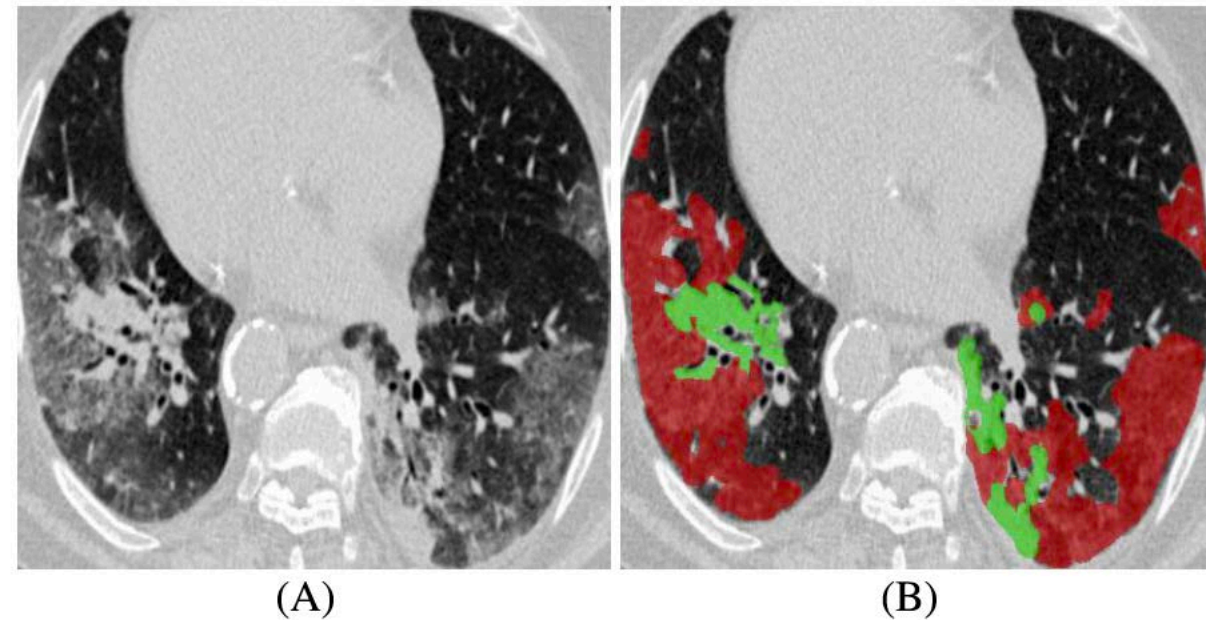


Fig. 1. Example of COVID-19 infected regions (B) in CT axial slice (A), where the red and green masks denote the GGO and consolidation, respectively. The images are collected from [9].

Segmenting infected regions from CT slices faces several challenges:

- High variation in infection characteristics
- Low intensity contrast between infections and normal tissues

COVID-19 CT Image Segmentation

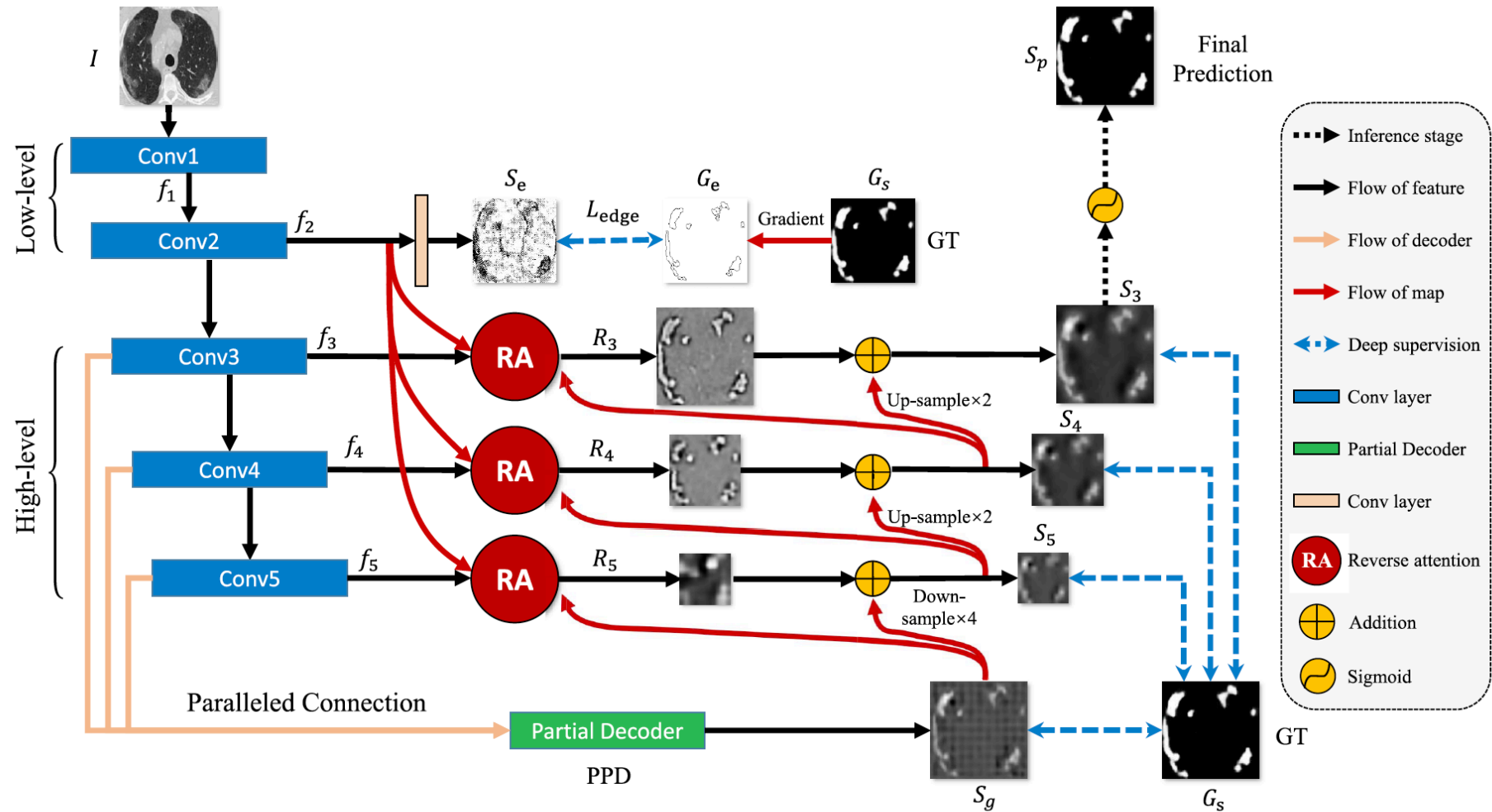
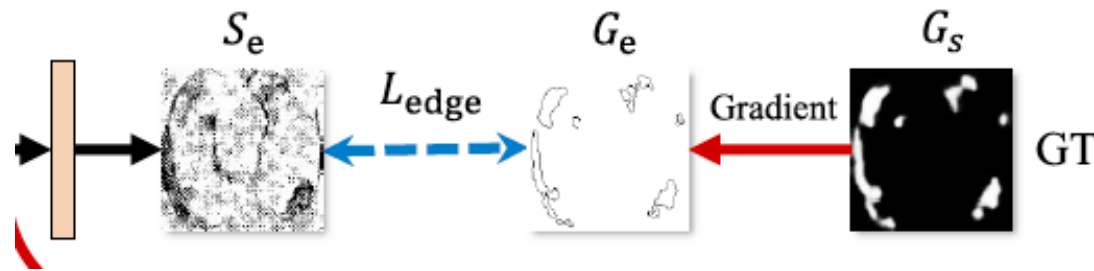


Fig. 2. The architecture of our proposed *Inf-Net* model, which consists of three reverse attention (RA) modules connected to the paralleled partial decoder (PPD). See § III-A for details.

COVID-19 CT Image Segmentation

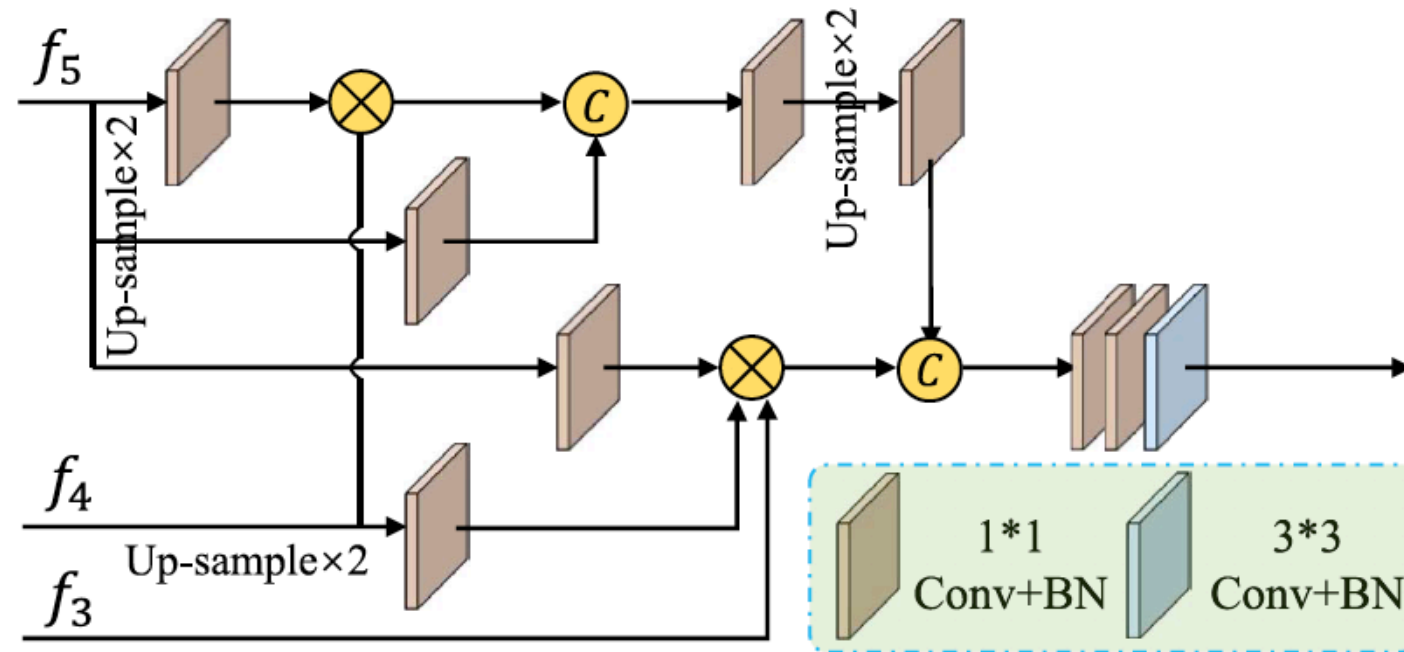
Edge Attention Module (EAM)



$$\mathcal{L}_{edge} = - \sum_{x=1}^w \sum_{y=1}^h [G_e \log(S_e) + (1 - G_e) \log(1 - S_e)],$$

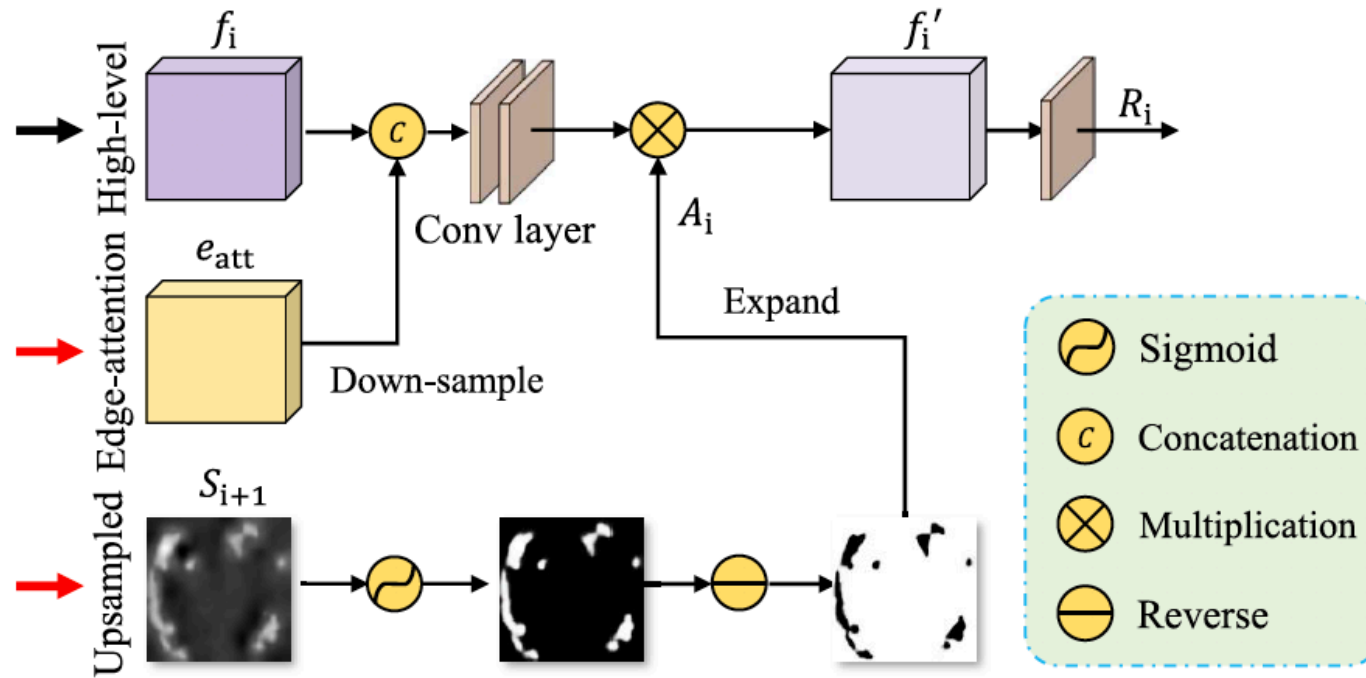
COVID-19 CT Image Segmentation

Paralleled partial decoder (PPD)



COVID-19 CT Image Segmentation

Reverse attention module (RAM)

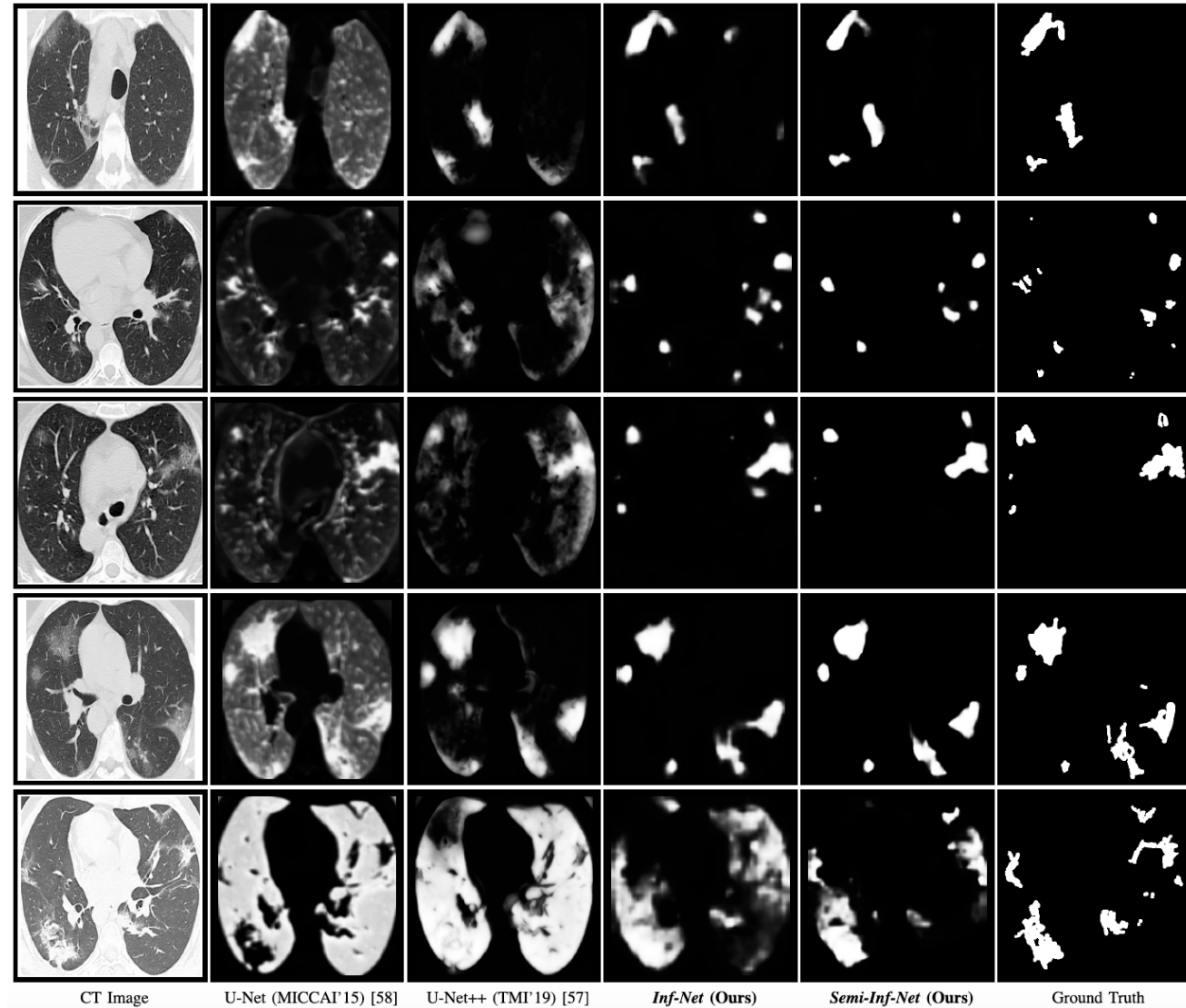


Results

TABLE IV

ABLATION STUDIES OF OUR *Semi-Inf-Net*. THE BEST TWO RESULTS ARE SHOWN IN RED AND BLUE FONTS

Methods	Dice	Sen.	Spec.	S_{α}	E_{ϕ}^{mean}	MAE
(No.1) Backbone	0.442	0.570	0.825	0.651	0.569	0.207
(No.2) Backbone+EA	0.541	0.665	0.807	0.673	0.659	0.205
(No.3) Backbone+PPD	0.669	0.744	0.880	0.720	0.810	0.125
(No.4) Backbone+RA	0.625	0.826	0.809	0.668	0.736	0.177
(No.5) Backbone+RA+EA	0.672	0.754	0.882	0.738	0.804	0.122
(No.6) Backbone+PPD+RA	0.655	0.690	0.927	0.761	0.812	0.098
(No.7) Backbone+PPD+RA+EA	0.739	0.725	0.960	0.800	0.894	0.064





<https://www.anaconda.com/>



<https://pytorch.org/>